

Synthesis of Uranium(VI) Terminal Oxo Complexes: Molecular Geometry Driven by the Inverse *Trans*-Influence

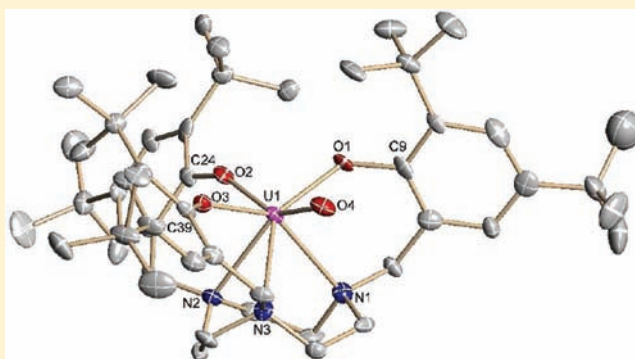
Boris Kosog,[†] Henry S. La Pierre,[†] Frank W. Heinemann,[†] Stephen T. Liddle,[‡] and Karsten Meyer^{*,†}

[†]Inorganic Chemistry, Department of Chemistry and Pharmacy, Friedrich-Alexander-University of Erlangen-Nuremberg, Egerlandstrasse 1, 91058 Erlangen, Germany

[‡]School of Chemistry, University of Nottingham, University Park, Nottingham NG7 2RD, U.K.

S Supporting Information

ABSTRACT: Oxidation of our previously reported uranium(V) oxo complexes, supported by the chelating (^RArO)₃tacn³⁻ ligand system (R = *tert*-butyl (*t*-Bu), **1-*t*-Bu**; R = 1-adamantyl (Ad), **1-Ad**), yields terminal uranium(VI) oxo complexes [((^RArO)₃tacn)U(VI)(O)]SbF₆ (R = *t*-Bu, **2-*t*-Bu**; R = Ad, **2-Ad**). These complexes differ in their molecular geometry in that **2-*t*-Bu** possesses pseudo-C_s symmetry in solution and solid state as the terminal oxo ligand lies in the equatorial plane (as defined by the three aryloxo arms of the ligand) in order to accommodate the thermodynamic preference of high-valent uranium oxo complexes to have a σ- and π-donating ligand *trans* to the oxo (*vis-à-vis* the ubiquity of the linear UO₂²⁺ moiety). The distortion of the ligand — which stands in contrast to all other complexes of uranium supported by the (^RArO)₃tacn³⁻ ligand, including **2-Ad** — is most clearly seen in the structures of **2-*t*-Bu**, [((^t-BuArO)₃tacn)U(VI)(O)_{eq}]SbF₆, and **3-*t*-Bu**, [((^t-BuArO)₃tacn)U(VI)(O)_{eq}(OC(O)CF₃)_{ax}]. The solid-state structure of **3-*t*-Bu** reveals that the *trans* U—O_{ArO} bond length is shortened by 0.1 Å in comparison to the *cis* U—O_{ArO} bonds and the *trans* U—O—C_{ipso} angle is linearized (157.67° versus 147.85° and 130.03°). Remarkably, the minor modification of the ligand to have Ad groups at the *ortho* positions of the aryloxo arms is sufficient to stabilize a C_{3v}-symmetric terminal uranium(VI) oxo complex (**2-Ad**) without a ligand *trans* to the oxo. These experimental results were reproduced in DFT calculations and allow the qualitative bracketing of the relative thermodynamic stabilization afforded by the inverse *trans*-influence as ~6 kcal mol⁻¹.



INTRODUCTION

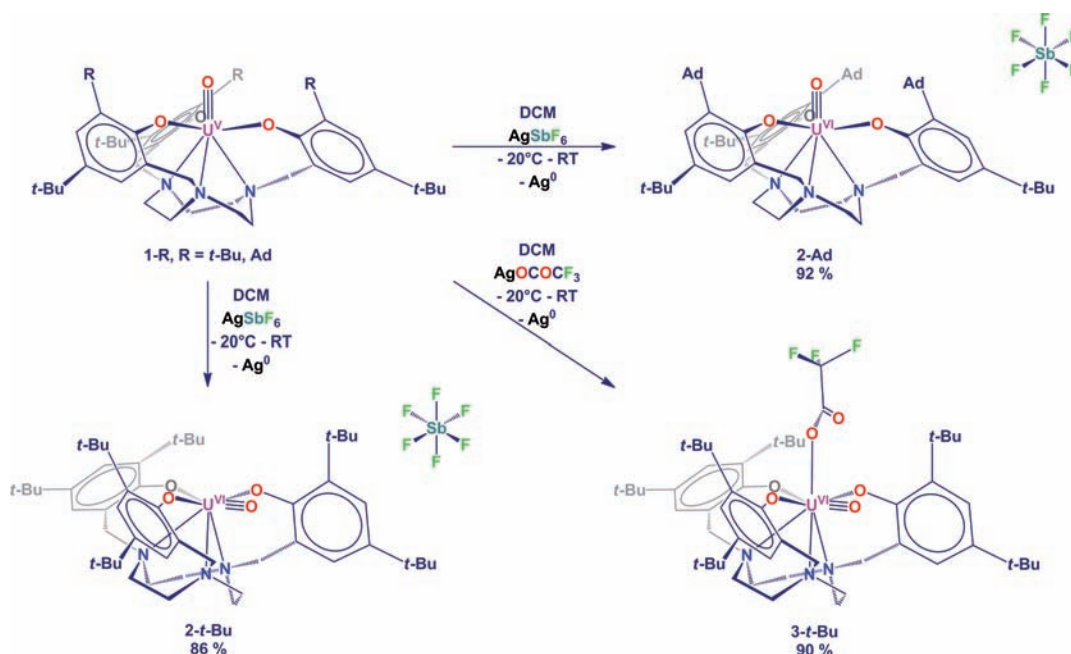
The uranyl *trans*-dioxo moiety [O=U=O]²⁺ is the predominant chemical feature of extant molecular uranium complexes.¹ Given the central importance of uranium as a nuclear fuel, significant theoretical and experimental work has been pursued to understand the unusual electronic structure of uranyl,^{1,2} which is strikingly dissimilar from that of the analogous transition metal dioxo complexes. While such questions of electronic and molecular structure are central to the further development of bonding theory and coordination chemistry, they are also important to the development of essential technologies — namely, methods for uranyl sequestration and chemical remediation. Recent reports have documented significant progress towards both goals.³ In this context, it is remarkable that terminal uranium(VI) mono-oxo complexes remain an exceedingly rare class of compounds.⁴ The coordination chemistry and reactivity of these complexes are governed by their unique electronic structure. This structure is analogous to the valence-core orbital mixing that drives the thermodynamic stability of uranyl.^{2a,5} In this article we report the synthesis and characterization of uranium(VI) mono-oxo complexes in order to further address these issues.

We previously reported the synthesis of uranium(V) terminal mono-oxo complexes via multiple-bond metathesis of a high-valent uranium(V) mesitylimido complex with CO₂.^{4d} These uranium(V) oxo complexes were obtained for two different ligands, both consisting of a triazacyclononane (tacn) backbone with three aryloxo arms (^RArO)₃tacn³⁻ with different *ortho* substituents R (R = *tert*-butyl (*t*-Bu), **1-*t*-Bu**; R = adamantyl (Ad), **1-Ad**). These seven-coordinate complexes, as for most of the tacn-based compounds, present with axial coordination of the oxo ligand. This arrangement forms a trigonal pyramidal coordination of the oxygen atoms around the uranium core. Thus, the compounds are C_{3v} symmetric. Given the unusual structural features of the only two crystallographically characterized uranium(VI) mono-oxo complexes known at the start of our studies, ([UCl₅O][PPh₄])^{4a} and [Cp*₂U(NAr)(O)], Ar = 2,6-diisopropylphenyl,^{4b} we were motivated to explore the oxidation of complexes **1-*t*-Bu** and **1-Ad**.

Received: December 13, 2011

Published: February 24, 2012

Scheme 1. Oxidation of $[((^R\text{ArO})_3\text{tacn})\text{U}(\text{V})\text{O}]$ (**1-R**) with 1 equiv of AgSbF_6 to give $[((^R\text{ArO})_3\text{tacn})\text{U}(\text{VI})\text{O}]\text{SbF}_6$ (**2-R**) or 1 equiv of $\text{AgOC}(\text{O})\text{CF}_3$ to form $[((^{t\text{-Bu}}\text{ArO})_3\text{tacn})\text{U}(\text{VI})\text{O}]_e\text{q}(\text{OC}(\text{O})\text{CF}_3)_{\text{ax}}$ (**3-*t*-Bu**)



RESULTS AND DISCUSSION

Initial studies of the U(V) oxo complexes (**1-*t*-Bu** and **1-Ad**) by cyclic voltammetry revealed a reversible oxidation to uranium(VI) at -0.13 V vs Fc^+/Fc for **1-*t*-Bu** and -0.19 V vs Fc^+/Fc for **1-Ad** (see Supporting Information). Chemical oxidation of an orange-red solution of **1-*t*-Bu** in methylene chloride with 1 equiv of AgSbF_6 afforded, after workup, 86% yield of **2-*t*-Bu** as a deep black powder (Scheme 1). In contrast to the cleanly reversible electrochemical oxidation, solution structural studies indicated that chemical oxidation led to the isolation of a structurally rearranged product. It presents with pseudo- C_s symmetry as seen in, and supported by, its diamagnetic ^1H NMR spectrum in benzene- d_6 . Most telling, the aryloxy arms are no longer equivalent — rather the appropriate resonances are split in an approximate 2:1 ratio indicating the arms are related by a mirror plane.⁶ The oxidation state assignment as U(VI) was further confirmed by visible spectroscopy, which lacked any features attributable to metal-based $f-f$ transitions (see Supporting Information). This structural assignment was corroborated, reproducibly, by an X-ray diffraction (XRD) study, which confirmed that the complex is hepta-coordinate with the terminal oxo *trans* to an aryloxy and a non-coordinating SbF_6^- anion (Figure 1).⁷

In order to explore the role of a potentially coordinating anion in determining the oxo coordination mode, the oxidation of **1-*t*-Bu** by $\text{AgOC}(\text{O})\text{CF}_3$ was performed. The complex $[((^{t\text{-Bu}}\text{ArO})_3\text{tacn})\text{U}(\text{VI})\text{O}]_e\text{q}(\text{OC}(\text{O})\text{CF}_3)_{\text{ax}}$ (**3-*t*-Bu**) was obtained in 90% yield as a black-brown powder (Scheme 1). The ^1H NMR spectrum of **3-*t*-Bu** is similar to that of **2-*t*-Bu**, but in this case all three arms have different chemical environments.⁸ Crystallization of **3-*t*-Bu** by slow diffusion of *n*-hexane into a concentrated solution of **3-*t*-Bu** in a mixture of 1,2-dimethoxyethane (DME) and benzene gave single crystals of **3-*t*-Bu-DME** suitable for a crystallographic study (Figure 2). The only significant connectivity difference between that of **2-*t*-Bu** and **3-*t*-Bu** is that the supporting anion ($\text{F}_3\text{C}(\text{O})\text{CO}^-$)

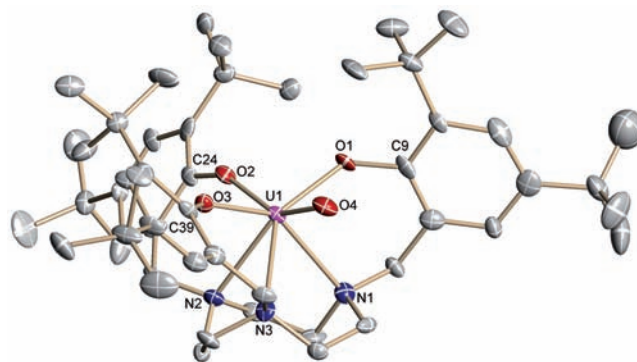


Figure 1. Solid-state molecular structure of one of two independent molecules of $[((^{t\text{-Bu}}\text{ArO})_3\text{tacn})\text{U}(\text{VI})\text{O}]_e\text{q}]\text{SbF}_6$ in crystals of $[((^{t\text{-Bu}}\text{ArO})_3\text{tacn})\text{U}(\text{VI})\text{O}]_e\text{q}]\text{SbF}_6 \cdot 3.5 \text{C}_6\text{H}_6$ (**2-*t*-Bu**·3.5 C_6H_6). The non-coordinating anion, co-crystallized solvents, and hydrogen atoms are removed for clarity. Thermal ellipsoids are at 50% probability. Selected bond lengths (Å) and angles (°): U1–O4, 1.836(6); U1–O2, 2.063(5); U1–O3, 2.092(6); U1–O1, 2.154(5); O4–U1–O2, 148.6(2); C9–O1–U1, 125.0(5); C24–O2–U1, 152.9(4); C39–O3–U1, 141.5(5).

is bound to the metal in the axial site, yielding a pseudo- C_s -symmetric octa-coordinate complex.

At first examination, the solid-state structures of **2-*t*-Bu** and **3-*t*-Bu** appear superimposable. The bond lengths of the terminal uranium oxo ligands are similar, at 1.836(6) and 1.820(6) Å (**2-*t*-Bu**)⁹ and 1.811(2) Å (**3-*t*-Bu**), and are both slightly shortened compared to the bond length of the uranium(V) precursor, which is 1.848(8) Å.^{4d} These bond lengths reasonably agree with those of the previously characterized uranium(VI) terminal oxo compounds: du Preez's $[\text{U}(\text{O})\text{Cl}_5][\text{PPh}_4]$, $\text{U}=\text{O} = 1.76(1)$ Å; Burns's $[\text{Cp}^*\text{U}(\text{O})(\text{NAr})]$, $\text{U}=\text{O} = 1.844(4)$ Å; and Hayton's most recently reported $[(\kappa^2\text{-CH}_2\text{SiMe}_2\text{NSiMe}_3)(\text{N}(\text{SiMe}_3)_2)_2\text{U}(\text{O})]$, $\text{U}=\text{O} = 1.800(2)$ Å.^{4d}

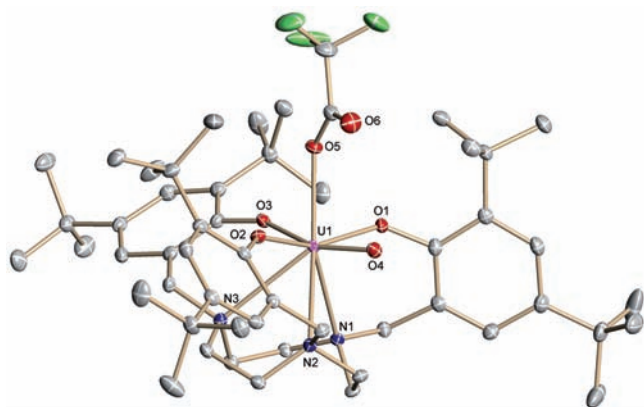


Figure 2. Solid-state molecular structure of $[(t\text{-BuArO})_3\text{tacn}]\text{U}(\text{VI})\text{(O)}_{\text{eq}}(\text{OC}(\text{O})\text{CF}_3)_{\text{ax}}$ in crystals of $[(t\text{-BuArO})_3\text{tacn}]\text{U}(\text{VI})\text{(O)}_{\text{eq}}(\text{OC}(\text{O})\text{CF}_3)_{\text{ax}}\cdot\text{DME}$ (**3-*t*-Bu·DME**). Co-crystallized solvent and hydrogen atoms are removed for clarity. Thermal ellipsoids are at 50% probability. Selected bond lengths (Å) and angles ($^\circ$): U1–O4, 1.811(2); U1–O3, 2.058(2); U1–O2, 2.140(2); U1–O1, 2.161(2); U1–O5, 2.350(2); O4–U1–O3, 159.67(6); C9–O1–U1, 130.0(2); C24–O2–U1, 147.9(2); C39–O3–U1, 157.7(2).

However, on closer inspection the two structures differ in crucial aspects. The most striking feature of seven-coordinate **2-*t*-Bu** and eight-coordinate **3-*t*-Bu** is that the terminal oxo is displaced towards (**2-*t*-Bu**) or lies in the equatorial plane (**3-*t*-Bu**) (as defined by the aryloxy arms of the ligand). The geometric distortion created in the ligand is most pronounced in **3-*t*-Bu**. One aryloxy arm is *trans* to the oxo (O4–U1–O3, 159.67(6) $^\circ$), and the other two are disposed *cis* (O4–U1–O2, 89.26(6) $^\circ$; O4–U1–O1, 80.30(6) $^\circ$; sum of angles around U1 in equatorial plane = 355.06 $^\circ$). The *trans*-aryloxy U1–O3 bond length, 2.058(2) Å, is about 0.1 Å shorter than the bond lengths of the *cis*-aryloxides: the U1–O1 and U1–O2 bond distances are 2.161(2) and 2.140(2) Å, respectively. To the best of our knowledge, this phenomenon has been experimentally observed and reported only once previously in a uranium system, namely $[\text{UOCl}_5][\text{PPh}_4]$.^{4a} Similarly, in this complex the *trans* U–Cl bond is 0.103(3) Å shorter than the *cis* U–Cl bonds. This anomalous structural feature was originally rationalized by using an ionic, ligand–ligand repulsion model, whereby the *trans* chloride would experience the least repulsion.^{4a} More modern treatments, based on molecular orbital theory, labeled the inverse *trans*-influence (ITI) by Denning,^{2d} invoke the participation of core 6p orbitals via hybridization with the valence 5f orbitals, which have the same parity.^{5a,b} This argument is similar to that developed for rationalizing the preference of uranyl to adopt a linear geometry, and the involvement of the 6p core orbitals has been shown both theoretically and experimentally.^{2a,d} While the exact mechanism by which the 6p orbitals affect the ITI and whether other factors play a role remain open to debate, the total thermodynamic stabilization due to the ITI has been estimated (by consideration of crystal packing forces) to be >1 kcal mol⁻¹.¹⁰

In this context, it is revealing to further examine the U–O–C_{ipso} bond angles in the structure of **3-*t*-Bu**. The *trans*-aryloxy is disposed nearly linearly from the uranium center with a U1–O3–C39 angle of 157.7(2) $^\circ$. This angle is in contrast to the much more acute angles of the *cis*-aryloxides (U1: U1–O2–C24, 147.9(2) $^\circ$; U1–O1–C9, 130.0(2) $^\circ$). Aryloxides, like siloxides and alkoxides, are pseudo-isolobal with oxos, imides, and

cyclopentadienide ligands in that they can all act as 1 σ -,2 π -donors.¹¹ The linearity of this *trans* U–O–C_{ipso} bond angle, in analogy to arguments established for the bonding of linear imides,¹² is indicative (but not conclusive) of π donation of the *trans*-aryloxy to the uranium center. It has been phenomenologically observed that M–O–C_{ipso} bond lengths and angles do not correlate for electron-deficient early transition metals and lanthanides, which suggests that the potential well to distort this angle is very shallow and that the bond is largely electrostatic.¹³ For the complexes reported herein, the correlation between the shortened U–O bond and the linearized U–O–C_{ipso} bond angle implies that increased π donation may be the basis of this phenomenon (not just a steric interaction).¹⁴

Thus, it is tantalizing to consider that the electronic basis of this observed ITI may be derived from not just hybridization of the core 6p_z (Z axis defined along the uranium-oxo axis) orbital (which has been rationalized to provide the basis of ITI via primarily key σ -bonding orbitals), but also π interactions generated by the appropriate hybridization of the 6p_x and 6p_y orbitals with the valence 5f orbitals. In this regard, the driving force for the equatorial oxo may be derived from the ability to adopt a uranyl-like geometry, as similar π interactions have been proposed as key, albeit small, components of the stabilization of linear uranyl.^{2a} Further crystallographic evidence for such an argument may be derived by considering the bond lengths in Hayton's complex, $[(\kappa^2\text{-CH}_2\text{SiMe}_2\text{NMe}_3)(\text{N}(\text{SiMe}_3)_2)_2\text{U}(\text{O})]$.^{4d} The U–C bond lies *trans* to the uranium terminal oxo; however, the ability to form significant π bonds is absent, and this bond is not significantly shorter than the expected bond length for a σ U(VI)–C bond (2.319(2) (XRD) vs 2.353–2.377 Å (DFT)).^{4c} The description of the crystallographic structure of **3-*t*-Bu** is completed by noting that the supporting tacn framework undergoes distortion to accommodate the electronic preferences of the uranium(VI) oxo: in the U–N distances, U1–N3 (N3 is the tacn-N, where the *trans*-aryloxy is attached) is the longest bond at 2.818(2) Å, while U1–N1 and U1–N2 are significantly shorter by about 0.11 Å, at 2.692(2) and 2.696(2) Å, respectively.

Complex **2-*t*-Bu**, in contrast to **3-*t*-Bu**, undergoes more subtle changes to accommodate an equatorial oxo ligand. Most important to note, the O_{oxo}–U–O_{transArO} in **2-*t*-Bu** is more acute and very much nonlinear (O4–U1–O2, 148.6(2) $^\circ$; O8–U2–O6, 149.5(2) $^\circ$ in **2-*t*-Bu** vs O4–U1–O3, 159.67(6) $^\circ$ in **3-*t*-Bu**). As a result, the uranium center in **2-*t*-Bu** lies significantly below the plane defined by the supporting aryloxy oxygen atoms of the ligand (U1, 0.735(4) Å and U2, 0.710(4) Å; Figure 3). This effect is also demonstrated by considering the sum of angles around U1 in equatorial plane is 338.8 $^\circ$ (sum of angles around U2 in equatorial plane = 339.7 $^\circ$). As a result, **2-*t*-Bu** does not present the ITI. The *trans*-aryloxy U1–O2 bond length, 2.063(5) Å, is approximately the same as the *cis*-aryloxides: the U1–O1 and U1–O3 bond distances are 2.154(5) and 2.092(6) Å, respectively (*trans*, U2–O6, 2.066(5) Å; *cis*, U2–O7, 2.064(6) Å and U2–O5, 2.123(6) Å).

This pattern is reproduced in the DFT analysis of **2-*t*-Bu** (*vide infra*). However, as in **3-*t*-Bu**, the *trans*-aryloxy is disposed from the uranium center with a wide U1–O2–C24 angle of 152.9(4) $^\circ$ (U2–O6–C75: 152.9(5) $^\circ$). This angle is in contrast to the much more acute angles of the *cis*-aryloxides (U1: U1–O3–C39, 141.5(5) $^\circ$; U1–O1–C9, 125.0(5) $^\circ$; U2: U2–O5–C60, 123.8(5) $^\circ$; U2–O7–C90, 141.6(6) $^\circ$). As in **3-*t*-Bu**, the linearly disposed *trans*-aryloxy may indicate π

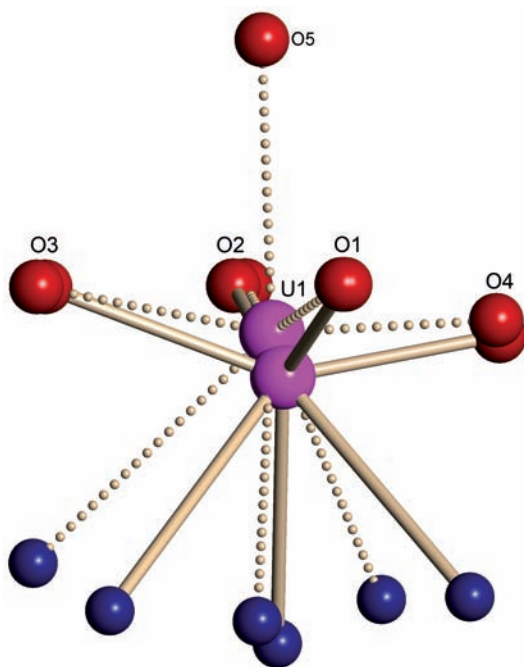


Figure 3. Overlay of core geometries of $2\text{-}t\text{-Bu}\cdot 3.5\text{C}_6\text{H}_6$ (solid bonds) and $3\text{-}t\text{-Bu}\cdot \text{DME}$ (dotted bonds).

bonding and overall suggests that, for both $2\text{-}t\text{-Bu}$ and $3\text{-}t\text{-Bu}$, the thermodynamic driving force for the equatorial distortion of the oxo ligand derives from the ability to adopt a uranyl-like geometry. In $3\text{-}t\text{-Bu}$, the coordination of $(\text{F}_3\text{C}(\text{O})\text{CO}^-)$ linearizes the $\text{O}_{\text{oxo}}\text{-U-O}_{\text{trans-ArO}}$ angle ($159.67(6)^\circ$) by pulling the U ion into the plane of the coordinating oxygens (U1, $0.3802(8)$ Å displacement below the plane defined by the three aryloxy oxygens; Figure 3). Therefore, $3\text{-}t\text{-Bu}$ has the correct geometry for the σ - and π -orbitals of the *trans*-aryloxy to mix with the valence 5f and core 6p orbitals to generate the observed ITI. Complex $2\text{-}t\text{-Bu}$, absent this axial ligand and further displaced from the aryloxy oxygen plane, does not present with a strong ITI. As with $3\text{-}t\text{-Bu}$, the tacn supporting framework of $3\text{-}t\text{-Bu}$ undergoes distortion to accommodate the equatorial oxo, wherein the longest U–N distance belongs to the tacn-N attached to *trans*-aryloxy arm (U1–N2, $2.643(6)$ Å; U(2)–N(5), $2.651(6)$ Å). However, the other two U–N distances (U1: U1–N1, $2.542(7)$ Å; U1–N3, $2.604(7)$ Å; U2: U2–N4, $2.557(7)$ Å; U2–N6, $2.599(7)$ Å) are not as similar as they are in $3\text{-}t\text{-Bu}$.

Given the demonstrated thermodynamic preference of uranium(VI) oxo supported by the $(^R\text{ArO})_3\text{tacn}^{3-}$ ligand system to adopt a uranyl-like geometry, it is surprising that the minor modification of the ligand to include Ad groups at the *ortho* positions of the aryloxides is sufficient to stabilize a uranium(VI) terminal oxo complex without a *trans* σ - and π -donating ligand. As indicated by the initial electrochemical studies of **1-Ad** (*vide supra*), the chemical oxidation of **1-Ad** with 1 equiv of AgSbF_6 in DCM affords $[(^{\text{Ad}}\text{ArO})_3\text{tacn}]\text{U}(\text{VI})(\text{O})\text{SbF}_6$ (**2-Ad**) as a deep black powder in 92% yield.¹⁵ Complex **2-Ad**, in contrast to $2\text{-}t\text{-Bu}$, presents with C_{3v} symmetry in solution — all aryloxy arms are equivalent.⁶ As with $2\text{-}t\text{-Bu}$, the oxidation state assignment was further confirmed by the absence of f–f transitions in the visible spectrum, as well as a SQUID measurement that supports its description as diamagnetic.

In order to gain further insight into the nature of $3\text{-}t\text{-Bu}$, we carried out restricted DFT calculations using a ZORA/TZP all-electron basis set on the whole molecule.¹⁶ The principal features of the experimentally determined structure of $3\text{-}t\text{-Bu}$ are reproduced well by the calculations (Table 1), and we thus

Table 1. Selected Experimental and Calculated Data for $3\text{-}t\text{-Bu}$

bond	expt (Å)	calc (Å)	bond order
U1–O1	2.1606(14)	2.192	1.21
U1–O2	2.1398(14)	2.176	1.28
U1–O3	2.0575(13)	2.120	1.35
U1–O4	1.8113(13)	1.826	2.64
U1–O5	2.3499(13)	2.324	0.81
U1–N1	2.6919(16)	2.836	0.35
U1–N2	2.6959(16)	2.828	0.34
U1–N3	2.8183(16)	2.971	0.29

conclude the calculations provide a qualitative description of the electronic structure of $3\text{-}t\text{-Bu}$. The calculated Mulliken charge for $3\text{-}t\text{-Bu}$ at uranium is $+2.67$, which shows significant charge donation from the ligands to uranium, and the aryloxy and oxo oxygen charges are -0.75 (av.) and -0.64 , respectively. The Nalewajski–Mrozek bond indices reveal a formal $\text{U}\equiv\text{O}$ triple bond and that the aryloxy oxygen centers are engaged in π -donation to uranium. Importantly, the trend of a short U–O bond *trans* to the oxo group compared to the two *cis* U–O aryloxy bonds are reproduced, as is the trend of one long and two short U–N bonds. There is extensive delocalization of the valence molecular orbitals across the calculated structure of $3\text{-}t\text{-Bu}$ due to the numerous π and lone pair orbitals; thus, it is unreasonable to expect that an examination of individual molecular orbitals will provide insight into the ITI effect, since many orbitals in the manifold could contribute to it.

To deconvolute the steric and electronic effects of the $(\text{F}_3\text{C}(\text{O})\text{CO}^-)$ group in $3\text{-}t\text{-Bu}$ with respect to the ITI, we geometry optimized the structures of the corresponding cationic axial and equatorial oxo isomers $2\text{-}t\text{-Bu}^+_{\text{ax}}$ and $2\text{-}t\text{-Bu}^+_{\text{eq}}$ without the $(\text{F}_3\text{C}(\text{O})\text{CO}^-)$ group. For $2\text{-}t\text{-Bu}^+_{\text{ax}}$, the $\text{U}\equiv\text{O}$ and U–O bond distances were calculated to be 1.835 and 2.110, 2.136, and 2.155 Å. Importantly, the three U–O aryloxy bonds are now quite similar to each other. For $2\text{-}t\text{-Bu}^+_{\text{eq}}$, the corresponding $\text{U}\equiv\text{O}$ bond distance is shorter at 1.827 Å. Additionally, the U–O bonds now fall into two groups: the *trans* U–O bond is calculated to be 2.111 Å and the two *cis* U–O bonds are 2.150 and 2.178 Å (see Table 2). The calculated $\text{O}_{\text{trans}}\text{-U-O}_{\text{oxo}}$ and $\text{U-O-C}_{\text{ispo}}$ angles for $2\text{-}t\text{-Bu}^+_{\text{eq}}$ are 154.4 and 153.0° , which compares well to the corresponding experimental values of 149.5 and 152.9° ,

Table 2. Selected Experimental and Calculated Data for $2\text{-}t\text{-Bu}$

bond	expt (Å)	calc (Å)	bond order
U1–O1	2.154(5), 2.123(6)	2.178	1.28
U1–O2	2.063(5), 2.066(5)	2.111	1.42
U1–O3	2.092(6), 2.064(6)	2.150	1.36
U1–O4	1.836(6), 1.820(6)	1.827	2.67
U1–N1	2.542(7), 2.557(7)	2.648	0.43
U1–N2	2.643(6), 2.651(6)	2.786	0.42
U1–N3	2.604(7), 2.599(7)	2.665	0.44

respectively, for **2-*t*-Bu**. Thus, on moving from axial to equatorial, the U≡O and *trans* U–O bonds shorten, which can be attributed to the ITI. This effect is attenuated compared to **3-*t*-Bu**, which we suggest derives from the absence of an eighth axial ligand, which enforces a nearly coplanar relationship between the uranium center and the aryloxy oxygen atoms. The calculations reveal that the equatorial isomer is more stable than the axial isomer by 6.3 kcal mol⁻¹. This value represents the minimum stabilization for **3-*t*-Bu** but is representative of the magnitude of the stabilization; thus, it can be seen that sterically demanding substituents could easily stabilize an axial oxo isomer as experimentally and theoretically proven in **2-Ad**, where the axial isomer is more stable than an equatorial one by 5.1 kcal mol⁻¹, as found in the DFT calculations. Finally, **1-*t*-Bu** exhibits exclusively the axial isomer in common with the Ad derivative **1-Ad**. However, in **1-*t*-Bu** there is a greater electronic repulsion compared to **2-*t*-Bu** due to the f¹ nature of the former, which results in a longer U≡O bond; hence, the electronic ITI is overcome by steric effects.

CONCLUSION

In summary, we have synthesized three new examples of rare uranium(VI) terminal mono-oxo complexes via the oxidation of U(V) oxo precursors supported by the (R₃ArO)₃tacn³⁻ ligand system. The ITI was demonstrated to be a key thermodynamic driving force in the formation of an equatorial terminal oxo in the case of **3-*t*-Bu**. A careful analysis of available crystallographic data indicates that, heretofore unexpected, π interactions may be crucial components of the ITI. Complex **2-*t*-Bu** undergoes a similar but less pronounced distortion, but remarkably retains a vacant and easily accessible axial coordination site as is evidenced by the ready coordination of (F₃C(O)CO⁻) in **3-*t*-Bu**. The isolation of the stabilized terminal oxo, **2-Ad**, facilitated DFT analysis of the axial and equatorial isomers of these uranium oxos and provided the basis of a qualitative determination of the energetic gain obtained by distortion to an equatorial oxo to be ~6 kcal mol⁻¹. These complexes are valuable synthons for exploring the potential role of ITI in controlling chemical reactivity.

Furthermore, these results suggest that the synthesis of other desirable terminally bound functional groups (i.e., nitride, alkylidyne) at high-valent uranium centers would be more thermodynamically favorable in the presence of a ligand architecture incorporating a strong σ- and π-donating ligand in the *trans* position. Studies toward these ends are currently underway.

EXPERIMENTAL SECTION

Synthesis of [((^t-BuArO)₃tacn)U(VI)O_{eq}]SbF₆ (2-*t*-Bu**).** A 20 mL scintillation vial was charged with an orange-red solution of 0.207 g (0.20 mmol) of [((^t-BuArO)₃tacn)U(V)O] (**1-*t*-Bu**) in 10 mL of methylene chloride and cooled to -20 °C. While stirring, a solution of 0.069 g (0.20 mmol, 1.0 equiv) of silver hexafluoroantimonate in methylene chloride was added dropwise. The reaction mixture instantaneously turned black and was allowed to stir while warming to room temperature for 30 min. The dark grayish precipitate was filtered off over a Celite pad on a glass frit, which was washed with methylene chloride. The volatiles of the filtrate were removed *in vacuo* to give 0.220 g (0.17 mmol, 86%) of [((^t-BuArO)₃tacn)U(VI)O_{eq}]SbF₆ as a deep black-brown powder. Elemental analysis for C₅₁F₆H₇₈N₃O₄SbU, calcd/found [%]: C, 48.20/48.51; H, 6.19/6.13; N, 3.31/3.59. ¹H NMR, benzene-*d*₆, 400 MHz, δ [ppm]: 7.97 (br s, 1H, C_{ar}-H), 7.81 (br s, 2H, C_{ar}-H), 7.60 (br s, 1H, C_{ar}-H), 7.35 (br s, 2H, C_{ar}-H), 6.76 (br s, 1H, benzyl-H), 5.83 (br s, 1H, benzyl-H), 5.35

(br s, 1H, benzyl-H), 5.25 (br s, 1H, benzyl-H), 4.75 (br s, 1H, benzyl-H), 4.60–4.28 (m, 3H, 1 benzyl-H, 2 tacn-H), 4.16 (br s, 1H, tacn-H), 3.95 (br s, 1H, tacn-H), 3.88 (br s, 1H, tacn-H), 3.77–3.20 (m, 7H, tacn-H), 2.83 (br s, 1H, tacn-H), 2.10 (br s, 9H, *t*-Bu), 1.62 (br s, 9H, *t*-Bu), 1.50–1.23 (m, 36 H, *t*-Bu). IR, $\tilde{\nu}$ [cm⁻¹]: 2959 (vs), 2905 (s), 2868 (s), 1653 (vw), 1599 (w), 1560 (vw), 1550 (vw), 1476 (s), 1462 (s, br), 1443 (s), 1410 (w), 1393 (w), 1364 (m), 1306 (w), 1227 (s, br), 1201.7 (s), 1167 (vs), 1125 (s), 1094 (w, br), 1063 (w), 1026 (w, br), 947 (vw), 914 (w), 883 (w), 841 (s), 810 (m), 793 (w), 747 (m), 660 (vs, SbF₆), 610 (vw), 565 (vw), 542 (m), 507 (vw), 455 (m, br), 428 (w).

Synthesis of [((^{Ad}ArO)₃tacn)U(VI)O_{ax}]SbF₆ (2-Ad**).** A 20 mL scintillation vial was charged with an orange-red solution of 0.254 g (0.20 mmol) of [((^{Ad}ArO)₃tacn)U(V)O] (**1-Ad**) in 10 mL of methylene chloride and was cooled to -20 °C. While stirring, a solution of 0.069 g (0.20 mmol, 1.0 equiv) of silver hexafluoroantimonate in methylene chloride was added dropwise. The reaction mixture instantaneously turned black and was allowed to stir while warming to room temperature for 1 h. A dark grayish precipitate was filtered off over a Celite pad on a glass frit, which was washed with methylene chloride. The volatiles of the filtrate were removed *in vacuo* to give 0.277 g (0.18 mmol, 92%) of [((^{Ad}ArO)₃tacn)U(VI)O_{ax}]SbF₆ as a deep black-brown powder. Elemental analysis for C₆₉F₆H₉₆N₃O₄SbU·C₇H₈, calcd/found [%]: C, 57.14/56.82; H, 6.56/6.12; N, 2.63/2.71. ¹H NMR, benzene-*d*₆, 400 MHz, δ [ppm]: 7.89 (s, 3H, C_{ar}-H), 7.43 (s, 3H, C_{ar}-H), 5.92 (d, *J* = 13.4 Hz, 3H, benzyl-H), 5.24 (d, *J* = 13.4 Hz, 3H, benzyl-H), 4.17 (unres. dd, 3H, tacn-H), 3.83 (d, *J* = 14.0 Hz, 3H, tacn-H), 3.57 (unres. d, 3H, tacn-H), 3.35 (d, *J* = 14.0 Hz, 3H, tacn-H), 2.47 (q, *J* = 11.2 Hz, 18H, Ad-H), 2.07 (s, 6H, Ad-H), 1.98 (s, 3H, Ad-H), 1.79 (d, *J* = 11.2 Hz, 9H, Ad-H), 1.65 (d, *J* = 11.2 Hz, 9H, Ad-H), 1.34 (s, 27H, *t*-Bu). IR, $\tilde{\nu}$ [cm⁻¹]: 2951 (s), 2903 (vs, br), 2849 (s), 1597 (w), 1456 (s, br), 1449 (s), 1410 (w), 1397 (w), 1364 (m), 1344 (w), 1321 (w), 1308 (w), 1285 (w), 1259 (w), 1242 (w), 1202 (vs), 1126 (m), 1105 (m), 1094 (w), 1082 (w), 1063 (w), 1026 (w, br), 974 (w), 943 (vw), 918 (w), 880 (w), 839 (s), 806 (s), 787 (w), 772 (m), 748 (w), 731 (m), 694 (vw), 660 (vs, SbF₆), 642 (m), 596 (vw), 581 (vw), 567 (vw), 542 (m, br), 503 (vw), 484 (w), 475 (w), 465 (w), 448 (w), 426 (w).

Synthesis of [((^t-BuArO)₃tacn)U(VI)O_{eq}](OC(O)CF₃)_{ax}] (3-*t*-Bu**).** A 20 mL scintillation vial was charged with an orange-red solution of 0.104 g (0.10 mmol) of [((^t-BuArO)₃tacn)U(V)O] (**1-*t*-Bu**) in 5 mL of methylene chloride and was cooled to -20 °C. While stirring, a solution of 0.022 g (0.10 mmol, 1.0 equiv) of silver trifluoroacetate in methylene chloride was added dropwise. The reaction mixture quickly turned black-brown and was allowed to stir overnight at room temperature. The dark grayish precipitate was filtered off over a Celite pad on a glass frit, which was washed with methylene chloride. The volatiles of the filtrate were removed *in vacuo* to give 0.103 g (0.09 mmol, 90%) of [((^t-BuArO)₃tacn)U(VI)O_{eq}](OC(O)CF₃)_{ax}] as a deep black-brown powder. Elemental analysis for C₅₃F₃H₇₈N₃O₆U, calcd/found [%]: C, 55.44/55.48; H, 6.85/7.18; N, 3.66/3.83. ¹H NMR, benzene-*d*₆, 400 MHz, δ [ppm]: 8.11 (d, *J* = 2.2 Hz, 1H, C_{ar}-H), 7.96 (d, *J* = 2.2 Hz, 1H, C_{ar}-H), 7.68 (d, *J* = 2.2 Hz, 1H, C_{ar}-H), 7.33 (d, *J* = 2.2 Hz, 1H, C_{ar}-H), 7.21 (d, *J* = 2.2 Hz, 1H, C_{ar}-H), 6.80 (d, *J* = 2.2 Hz, 1H, C_{ar}-H), 6.36 (d, *J* = 14.1 Hz, 1H, benzyl-H), 5.39 (d, *J* = 12.8 Hz, 1H, benzyl-H), 5.04 (d, *J* = 11.0 Hz, 1H, benzyl-H), 4.62 (d, *J* = 12.8 Hz, 1H, benzyl-H), 3.67 (d, *J* = 13.6 Hz, 1H, benzyl-H), 3.61 (d, *J* = 11.4 Hz, 1H, benzyl-H), 3.44–3.26 (m, 2H, tacn-H), 3.26–3.12 (m, 2H, tacn-H), 3.04–2.84 (m, 2H, tacn-H), 2.85–2.63 (m, 2H, tacn-H), 2.55–2.20 (m, 2H, tacn-H), 2.05 (s, 9H, *t*-Bu), 1.99 (s, 9H, *t*-Bu), 1.65 (s, 9H, *t*-Bu), 1.41 (s, 9H, *t*-Bu), 1.35 (s, 9H, *t*-Bu), 1.16 (s, 9H, *t*-Bu). IR, $\tilde{\nu}$ [cm⁻¹]: 2958 (vs), 2905 (s), 2868 (s), 1782 (vw), 1707 (vs, U(CF₃)C=O), 1648 (w), 1601 (w), 1581 (vw), 1477 (s), 1466 (s), 1440 (s), 1409 (s), 1393 (s), 1363 (s), 1348 (w), 1308 (m), 1253 (m), 1235 (s, OC(O)CF₃), 1221 (vs), 1201 (vs), 1179 (vs, OC(O)CF₃), 1168 (vs), 1143 (s, OC(O)CF₃), 1126 (s), 1100 (m), 1103 (m), 1076 (m), 1025 (w), 1015 (w), 986 (vw), 948 (vw), 932 (vw), 916 (w), 890 (vw), 878 (m), 843 (s), 835 (s), 813 (m), 789 (m), 758 (w), 743 (m), 718 (m, OC(O)CF₃), 649 (vw), 605 (vw), 534 (m, br), 455 (m, br).

■ ASSOCIATED CONTENT

■ Supporting Information

General considerations, UV–vis spectra, crystallographic techniques and tables, electrochemical data, synthetic details for **4-*t*-Bu**, and computational details for **2-*t*-Bu**, **2-Ad**, and **3-*t*-Bu** (PDF, CIF). This material is available free of charge via the Internet at <http://pubs.acs.org>.

■ AUTHOR INFORMATION

Corresponding Author

karsten.meyer@chemie.uni-erlangen.de

Notes

The authors declare no competing financial interest.

■ ACKNOWLEDGMENTS

This research was supported by grants from the German Bundesministerium für Bildung und Forschung (BMBF project 02NUK012C), and DFG through SFB 583. The FAU Erlangen-Nuremberg is gratefully acknowledged for financial support as is COST Action CM1006. S.T.L. thanks the Royal Society, EPSRC, ERC, and University of Nottingham for support. The authors thank Oanh P. Lam (Lawrence Berkeley National Laboratory) for help with the crystallography of complex **2-*t*-Bu**.

■ REFERENCES

- (1) Zhang, Z. Y.; Pitzer, R. M. *J. Phys. Chem. A* **1999**, *103*, 6880.
- (2) (a) Tatsumi, K.; Hoffmann, R. *Inorg. Chem.* **1980**, *19*, 2656. (b) Wadt, W. R. *J. Am. Chem. Soc.* **1981**, *103*, 6053. (c) Pyykkö, P.; Laakkonen, L. J.; Tatsumi, K. *Inorg. Chem.* **1989**, *28*, 1801. (d) Denning, R. G. *Struct. Bonding (Berlin)* **1992**, *79*, 215. (e) Kaltsoyannis, N. *Inorg. Chem.* **2000**, *39*, 6009. (f) Denning, R. G.; Green, J. C.; Hutchings, T. E.; Dallera, C.; Tagliaferri, A.; Giarda, K.; Brookes, N. B.; Braicovich, L. *J. Chem. Phys.* **2002**, *117*, 8008. (g) Matsika, S.; Pitzer, R. M. *J. Phys. Chem. A* **2001**, *105*, 637.
- (3) (a) Beer, S.; Berryman, O. B.; Ajami, D.; Rebek, J. *Chem. Sci.* **2010**, *1*, 43. (b) Sather, A. C.; Berryman, O. B.; Rebek, J. *J. Am. Chem. Soc.* **2010**, *132*, 13572. (c) Arnold, P. L.; Hollis, E.; White, F. J.; Magnani, N.; Caciuffo, R.; Love, J. B. *Angew. Chem., Int. Ed.* **2011**, *50*, 887. (d) Arnold, P. L.; Pecharman, A. F.; Hollis, E.; Yahia, A.; Maron, L.; Parsons, S.; Love, J. B. *Nature Chem.* **2010**, *2*, 1056. (e) Arnold, P. L.; Patel, D.; Wilson, C.; Love, J. B. *Nature* **2008**, *451*, 315. (f) Lovley, D. R.; Phillips, E. J. P.; Gorby, Y. A.; Landa, E. R. *Nature* **1991**, *350*, 413. (g) Nocton, G.; Horeglad, P.; Vetere, V.; Pecaut, J.; Dubois, L.; Maldivi, P.; Edelstein, N. M.; Mazzanti, M. *J. Am. Chem. Soc.* **2010**, *132*, 495. (h) Natrajan, L.; Burdet, F.; Pecaut, J.; Mazzanti, M. *J. Am. Chem. Soc.* **2006**, *128*, 7152. (i) Berthet, J. C.; Thuery, P.; Ephritikhine, M. *Chem. Commun.* **2005**, 3415.
- (4) Molecular U(VI) terminal monooxo complexes: (a) de Wet, J. F.; du Preez, J. G. H. *J. Chem. Soc., Dalton Trans.* **1978**, 592. (b) Arney, D. S. J.; Burns, C. J. *J. Am. Chem. Soc.* **1995**, *117*, 9448. (c) Fortier, S.; Kaltsoyannis, N.; Wu, G.; Hayton, T. W. *J. Am. Chem. Soc.* **2011**, *133*, 14224. Molecular U(V) terminal monooxo complexes: (d) Bart, S. C.; Anthon, C.; Heinemann, F. W.; Bill, E.; Edelstein, N. M.; Meyer, K. *J. Am. Chem. Soc.* **2008**, *130*, 12536. (e) Arney, D. S. J.; Burns, C. J. *J. Am. Chem. Soc.* **1993**, *115*, 9840. See also ref 4c. Molecular U(IV) terminal monooxo complexes: (f) Zi, G. F.; Jia, L.; Werkema, E. L.; Walter, M. D.; Gottfriedsen, J. P.; Andersen, R. A. *Organometallics* **2005**, *24*, 4251. (g) Kraft, S. J.; Walensky, J.; Fanwick, P. E.; Hall, M. B.; Bart, S. C. *Inorg. Chem.* **2010**, *49*, 7620.
- (5) (a) O'Grady, E.; Kaltsoyannis, N. *J. Chem. Soc., Dalton Trans.* **2002**, 1233. (b) Straka, M.; Patzschke, M.; Pyykkö, P. *Theor. Chem. Acc.* **2003**, *109*, 332. (c) Chermette, H.; Rachedi, K.; Volatron, F. *J. Mol. Struct.: THEOCHEM* **2006**, *762*, 109.
- (6) VT NMR on **2-*t*-Bu** and **3-Ad** was performed. Complex **2-*t*-Bu** readily undergoes thermal isomerization. Coalescence of the aryl peaks is evident at just 30 °C. However, a number of rearrangement processes are extant, and the direct determination of thermodynamic parameters is not possible. Given the incipient isomerization observed at 30 °C, a lower barrier of ~10 kcal mol⁻¹ is likely. Complex **2-Ad** is poorly soluble at low temperature, and no resolution of isomers was observed down to -50 °C. See Supporting Information for further details.
- (7) X-ray-quality crystals of **2-*t*-Bu** can be obtained reproducibly, and a duplicate data set has been measured, which yields an identical assignment. See Supporting Information and CIF files for crystallographic details.
- (8) The oxidation of **1-*t*-Bu** was also accomplished with AgF in DCM to give a black powder, **4-*t*-Bu**, in 59% yield. This complex is analytically pure and spectroscopically similar to **3-*t*-Bu** based on its ¹H NMR and UV/vis spectra, implying that its solution connectivity is similar to that of **3-*t*-Bu**. See Supporting Information for full characterization.
- (9) Complex **2-*t*-Bu** crystallizes in the monoclinic space group *Cc* with two independent molecules of the complex and seven molecules of co-crystallized benzene in the asymmetric unit. Geometric parameters for the second independent molecule are included in text. See Supporting Information for further details.
- (10) Krinsky, J. L.; Minasian, S. G.; Arnold, J. *Chem.—Eur. J.* **2011**, *50*, 345.
- (11) Albright, T. A.; Burdett, J. K.; Whangbo, M. H. *Orbital Interactions in Chemistry*; Wiley: New York, 1985.
- (12) Wigley, D. E. *Prog. Inorg. Chem.* **1994**, *42*, 239. It should be noted that an argument for the bonding in early transition metal imides based on an electrostatic model has been proposed: Benson, M. T.; Bryan, J. C.; Burrell, A. K.; Cundari, T. R. *Inorg. Chem.* **1995**, *34*, 2348.
- (13) (a) Steffey, B. D.; Fanwick, P. E.; Rothwell, I. P. *Polyhedron* **1990**, *9*, 963. (b) Russo, M. R.; Kaltsoyannis, N.; Sella, A. *Chem. Commun.* **2002**, 2458. (c) Howard, W. A.; Trnka, T. M.; Parkin, G. *Inorg. Chem.* **1995**, *34*, 5900.
- (14) A similar argument has been proposed on the basis of reduction potentials of uranium(VI) aryloxide complexes: Fortier, S.; Wu, G.; Hayton, T. W. *Inorg. Chem.* **2009**, *48*, 3000.
- (15) The oxidation of **1-Ad** by AgOC(O)CF₃ or AgF gave complex mixtures. From these mixtures, the only isolable complexes were [((^{Ad}ArO)₃tacn)U(IV)(OC(O)CF₃)] and [((^{Ad}ArO)₃tacn)U(IV)(F)], respectively. See Supporting Information for crystallographic details.
- (16) The semicore 6p orbitals were not frozen in order to explore their role in ITI, as this phenomenon has already been well documented. See ref 5a.